1-16-2022

Tibetan Dust Accumulation Linked to Ecological and Landscape Response to Global Climate Change

Xianmei Huang
Shantou University and Purdue University

Xiaodong Miao
Linyi University, miaoxd109@yahoo.com

Qiufang Chang
Zhengzhou Normal University

Jiemei Zhong
Shantou University

Joseph A. Mason
University of Wisconsin-Madison, mason@wisc.edu

See next page for additional authors

AGU ADVANCING EARTH AND SPACE SCIENCE

Geophysical Research Letters®

RESEARCH LETTER
10.1029/2021GL096615

Tibetan Dust Accumulation Linked to Ecological and Landscape Response to Global Climate Change

Xianmei Huang[1,2], Xiaodong Miao[3], Qiufang Chang[4], Jiemei Zhong[1], Joseph A. Mason[5], Paul R. Hanson[6], Xianjiao Ou[7], Liubing Xu[8], and Zhongping Lai[1,9]

[1]Institute of Marine Sciences, Guangdong Provincial Key Laboratory of Marine Disaster Prediction and Protection, Shantou University, Shantou, China, [2]Department of Earth, Atmospheric and Planetary Sciences, Purdue University, West Lafayette, IN, USA, [3]Shandong Provincial Key Laboratory of Water and Soil Conservation and Environmental Protection, School of Resources and Environment, Linyi University, Linyi, China, [4]School of Geography and Tourism, Zhengzhou Normal University, Zhengzhou, China, [5]Department of Geography, University of Wisconsin-Madison, Madison, WI, USA, [6]Conservation and Survey Division, School of Natural Resources, University of Nebraska-Lincoln, Lincoln, NE, USA, [7]School of Geography and Tourism, Jiaying University, Meizhou, China, [8]Department of Geography, South China Normal University, Guangzhou, China, [9]School of Earth Sciences, China University of Geosciences, Wuhan, China

Abstract The Tibetan Plateau (TP) is a hotspot of earth system research, and understanding its landscape and ecosystem evolution has been hampered by the lack of time-constrained geological records. Geochronological data from 14 loess sites covering a large region in the Tibetan interior show that the TP loess, rather than accumulating during glacial periods, began aggrading at either 13.4 ± 0.4 or 9.9 ± 0.2 ka. An ecological threshold was crossed, when warmer and wetter conditions resulted in increased vegetation cover enabling dust trapping. This dust accumulation model is out of phase with that of the Chinese Loess Plateau (CLP) where high sedimentation rates occurred during the cold/dry glacial stages. The TP loess accumulation is in response to global climate change, at both orbital (glacial/interglacial) and millennial (e.g., Younger Dryas event) time scales, despite more complexity via ecological and landscape processes than the CLP loess.

Plain Language Summary It is very important to understand the processes of landscape and ecosystem evolution in Tibet to adapt to and mitigate the consequences from potential abrupt future climate changes, but not enough well-dated geological records are available. In this study, we present stratigraphic and numerical age results from 14 loess sites covering a large region in the Tibetan interior. Results show that Tibetan loess began aggrading at either 13.4 ± 0.4 or 9.9 ± 0.2 thousand years ago. Tibetan loess accumulated during warm/interglacial conditions of the Holocene and not during the last glacial period when loess aggradation rates in the Chinese Loess Plateau were high. In Tibet, vegetation cover, which was lowered during the last glacial period, increased during Holocene warming allowing for loess accumulation.

Xianmei Huang and Xiaodong Miao contributed equally.

Key Points:

- Numerical age results from 14 sites show that Tibetan loess started accumulation at either 13.4 ± 0.4 or 9.9 ± 0.2 ka
- Dust accumulation model of Tibetan landscape response to climate is out of phase with that in the Chinese Loess Plateau
- We provide an example of a teleconnection between ecological conditions in Tibet and Northern Hemisphere climate changes

Supporting Information:

Supporting Information may be found in the online version of this article.

Correspondence to:

X. Miao and Z. Lai,
Miaoxd109@yahoo.com;
zhongping.lai@yahoo.com

Citation:

Huang, X., Miao, X., Chang, Q., Zhong, J., Mason, J. A., Hanson, P. R., et al. (2022). Tibetan dust accumulation linked to ecological and landscape response to global climate change. *Geophysical Research Letters*, *49*, e2021GL096615. https://doi.org/10.1029/2021GL096615

Received 25 OCT 2021
Accepted 13 DEC 2021

Author Contributions:

Conceptualization: Zhongping Lai
Data curation: Xianmei Huang, Xiaodong Miao, Qiufang Chang, Xianjiao Ou, Liubing Xu, Zhongping Lai
Formal analysis: Xianmei Huang, Xiaodong Miao, Qiufang Chang, Zhongping Lai
Funding acquisition: Xiaodong Miao, Xianjiao Ou, Liubing Xu, Zhongping Lai
Investigation: Xianmei Huang, Xiaodong Miao, Qiufang Chang, Jiemei Zhong, Joseph A. Mason, Paul R. Hanson, Xianjiao Ou, Liubing Xu, Zhongping Lai
Methodology: Xianmei Huang, Xiaodong Miao, Paul R. Hanson, Zhongping Lai
Software: Joseph A. Mason, Xianjiao Ou

1. Introduction

Climate change affects ecosystems and landscapes through changes in mean conditions (e.g., slow solar insolation change) (Joshi et al., 2011; Steinbauer et al., 2018) and through rapid climatic events (Alley et al., 2003). A recent study has emphasized that it is critical to shift focus from target states to target rates of ecological change, distinguishing fast, slow and abrupt responses to climatic forcing (Williams et al., 2021), where abrupt responses are nonlinear, and related to thresholds and tipping points (Lenton et al., 2008). Past climate change, especially during the Late Quaternary with frequent abrupt climatic oscillations, provides an opportunity to identify hotspots of vulnerability and resilience and determine management interventions. In order to differentiate the fast-slow-abrupt response rates, however, one of the most critical prerequisites is the availability of well-dated climatic records for analysis of leads and lags, especially in places sensitive to climatic change like the Tibetan Plateau (TP).

The TP (Figure 1a) is a current hotspot of Earth system research, and the conservation status of the TP loess steppe ecoregion is expected to be vulnerable to changes in future warming scenarios (Beaumont et al., 2011). As one of the most sensitive areas to response to global climate change, warming in the TP occurred not only earlier based on modern observations (Liu & Chen, 2000), but also with large magnitude of temperature shifts based on climate modelling (Brown et al., 2020). Without understanding the processes and mechanisms of landscape and ecosystem evolution within the TP, it is challenging to adapt to and mitigate the consequences from

Supervision: Xiaodong Miao, Zhongping Lai
Validation: Joseph A. Mason, Zhongping Lai
Writing – original draft: Xianmei Huang, Xiaodong Miao
Writing – review & editing: Xianmei Huang, Xiaodong Miao, Jiemei Zhong, Joseph A. Mason, Paul R. Hanson, Xianjiao Ou, Liubing Xu, Zhongping Lai

potential abrupt future climate changes. However, independent of observed data and modeling, the paleoclimatic perspective on the impact of climate change on the TP ecosystem and landscape is very limited, and it has so far been hampered by the lack of time-constrained records to identify landscape responses to climate change over long periods of time.

Loess is a critical part of the TP ecosystem and landscape, as local Tibetans raise their livestock on the loess steppe in this vulnerable environment. Loess covers a large area on different types of landforms and provides important records of past changes in climate and landscape conditions. Loess in the TP is far less studied relative to its counterpart in the Chinese Loess Plateau (CLP), especially regarding its chronology (Stauch, 2015) and determining how changes in Northern Hemisphere climatic conditions impacted its aggradation through time.

Previous research has demonstrated a predominantly glacial origin of the silt in Tibetan loess, suggesting that it results from eolian sorting of glaciofluvial outwash deposits from braided river channels or alluvial fans (Sun et al., 2007). Optically stimulated luminescence (OSL) dating results reveal that loess accumulated episodically in the last 100 ka in the interior Tibet (Lai et al., 2009), although at the various TP margins basal ages of the loess can be much older, e.g., 127 ka in Ganzi (Yang et al., 2021) or even as old as 2 to 14 Ma in Xining (Lu et al., 2004). In summary, besides a few localized loess studies, there have not been systematic studies in the Tibetan interior that determine the conditions for loess accumulation and preservation.

Here we present loess stratigraphy and dating results from 14 sites distributed over a large region in the interior TP (Figure 1b; Figure S1 in Supporting Information S1) to address two main objectives. The first was to focus on deriving the basal age of loess deposits. The onset of dust accumulation represents a clear and dramatic change in landscape conditions that is easier to interpret relative to findings from most proxy-inferred changes. The second objective was to ascertain if the TP loess deposit includes evidence of globally recognized rapid climate changes as evident from other records in China (Dykoski et al., 2005; Y. Li et al., 2016; Porter & An, 1995). To do this, 57 OSL ages from 14 sites, augmented by a single radiocarbon age were generated to construct absolute chronologies to document regional loess deposition. In addition, grain-size data were generated from two selected loess sections to evaluate changes in environmental conditions.

2. Materials and Methods

2.1. Luminescence Dating

Luminescence dating procedures (Aitken, 1998) were conducted in the China University of Geosciences (Wuhan) and South China Normal University (Guangzhou). Sediments were treated with 10% HCl and 30% H_2O_2 to remove carbonate and organic matter. Samples were then wet sieved to obtain 38–63 or 90–125 μm grains, depending on the abundance of these grains in each sample. Samples with a grain size of 90–125 μm were etched with 40% HF for 60 min to remove feldspar minerals, while samples containing 38–63 μm grains were treated with 35% H_2SiF_6 for 2–3 weeks. Both were subsequently washed with 10% HCl for ~30 min to remove any precipitates. Grains from each sample were subjected to infrared stimulated luminescence (IRSL) to ensure purity of the quartz, and IRSL signals lower than 10% of the OSL signals are considered acceptable (Duller, 2003). Any samples with significant IRSL signals were retreated with HF or H_2SiF_6 to avoid age underestimation (Lai & Brueckner, 2008). Finally, the quartz sample was applied as a monolayer on the inner 0.6 cm of 0.97 cm diameter stainless-steel discs using silicone oil. OSL measurements were performed on a Risø TL/OSL-DA-20 reader equipped with a $^{90}Sr/^{90}Y$ beta source.

In order to select a suitable internal condition for equivalent dose (D_e) test, we conducted preheat plateau and dose recovery tests on samples CGS1-3, HTS1-C and QML2-1 (Figure S3 in Supporting Information S1). Preheat plateau tests show the paleodose of the three representative samples form an almost straight line from 220 to 260°C. As a result, a preheat temperature of 260°C for 10 s for natural and regenerative doses and cut heat at 220°C for 10 s for test dose were adopted for all samples. Meanwhile, a dose recovery test was carried out, using the Single Aliquot Regeneration (SAR) protocol (Murray & Wintle, 2000), with the ratios of measured dose to the given dose close to unity within 10% error. The OSL signals nearly decayed to the background level within 1–2 s, indicating dominance of the fast OSL signal component typical of quartz (Figure S4 in Supporting Information S1).

The D_e was determined by a combination of the SAR protocol (Murray & Wintle, 2000), and the standard growth curve (SGC) protocol (Lai, 2006; Roberts & Duller, 2004). Six aliquots from each sample were measured using

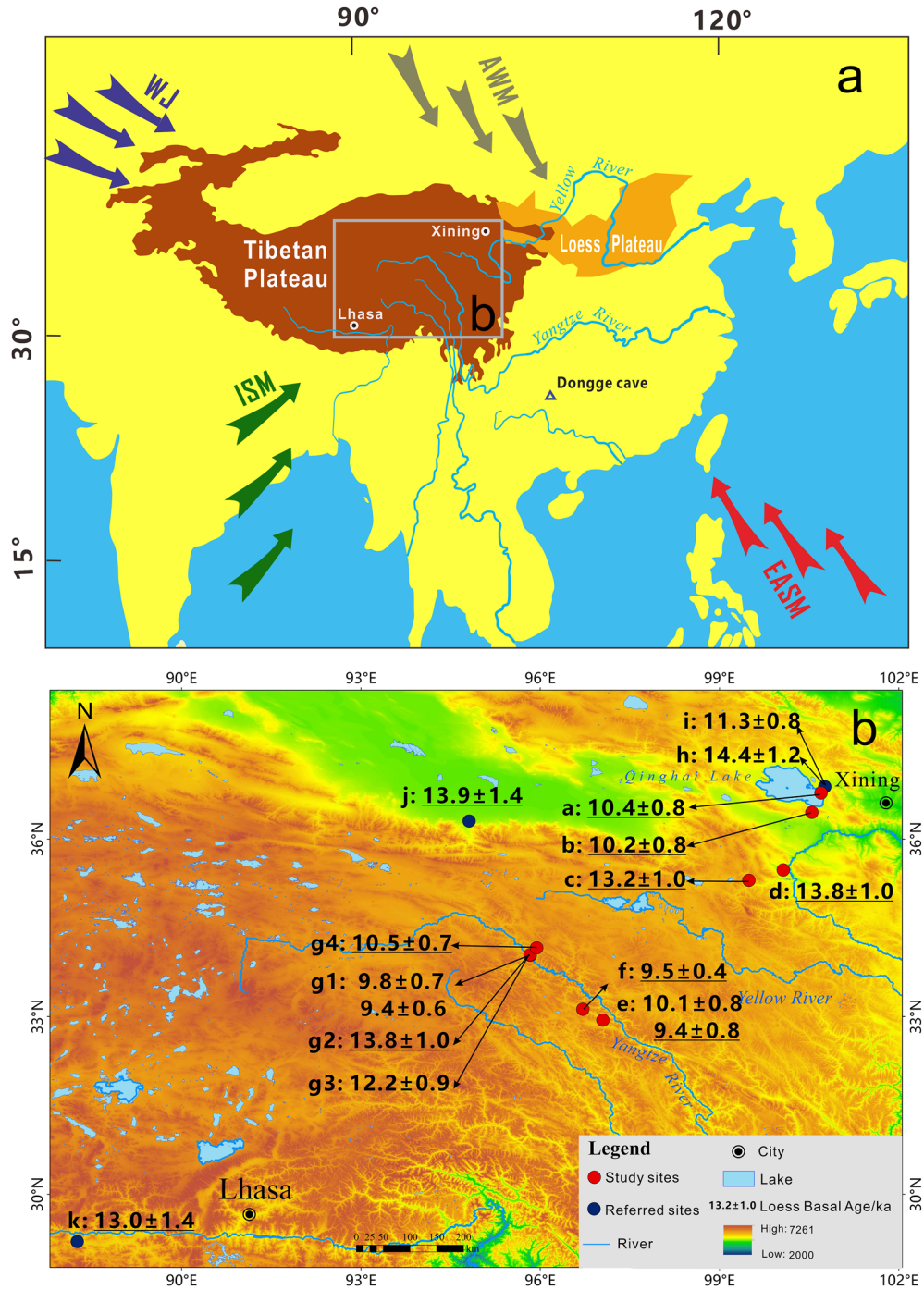

Figure 1. Study area of the Tibetan Plateau and sampling sites. (a), Location of the Tibetan Plateau (TP), Chinese Loess Plateau (CLP) and the four main atmospheric circulation systems that influence China: ISM (Indian Summer Monsoon), (WJ) Westerly jet, EASM (East Asian Summer Monsoon) and AWM (Asian Winter Monsoon). (b), Basal loess ages of each profile (two ages are shown if age reversal is present). Underlined ages denote that gravel layer was observed in the field, suggesting that the basal age is a close approximation of the onset of dust deposit; ages without underline denote that no gravel layer was observed, suggesting that the initial age of that site could be older. a, Xiangpishan; b, Xiala; c, Xinghai; d, Tongde; e, Changusi; f, Hongtushan; g1, Qumalai 1; g2, Qumalai 2; g3, Qumalai 3; g4, Qumalai 5; h, Bronze Wire site; i, Yandongtai (Sun et al., 2017); j, GEMH Xiaoganggou (Chen et al., 2011); k, TB8 (Sun et al., 2007). Detailed site information is in Table S1 in the Supporting Information S1.

the SAR protocol and an SGC curve was established based on the growth curves of the SAR data. To determine the natural signal (LN) and the test dose signal (TN), we measured additional 12 aliquots under the same measurement parameters. Each value of LN/TN was projected into the SGC curve to obtain a D_e value. Overdispersion values of four typical samples were calculated (Figure S5 in Supporting Information S1). The final D_e values are mostly considered as normally distributed and the central age model (Galbraith & Roberts, 2012) was used to calculate the final ages.

Neutron activation analysis was used to obtaining U, Th, and K for calculating the environmental dose rates. The cosmic ray dose was calculated based on the altitude, geographic location and depth of the samples (Prescott & Hutton, 1994). Water content was taken as 5 ± 3% for loess samples and 7 ± 3% for paleosol samples, based on the factors that the water contents for loess and paleosol samples from the CLP were given a value of 10 ± 5% and 15 ± 5%, respectively (Lai, 2010; Lai & Wintle, 2006), and that the precipitation in interior TP is less than that in the CLP. An alpha efficiency (α-value) of 0.035 ± 0.003 (Lai et al., 2008) was adopted for the 38–63 μm grains. The final dose rates were calculated with the "DRAC" program (Durcan et al., 2015). The OSL age was obtained by the age equation: OSL age (ka) = D_e (Gy)/Dose Rate (Gy/ka).

2.2. Radiocarbon Dating

A radiocarbon sample collected from bulk soil organic matter was taken from the Xinghai section at 1 m depth (Field ID: XH1-C; Lab ID: XA14512) and was analyzed at the radiocarbon laboratory within the Institute of Earth Environment, Chinese Academy of Sciences (Xi'an). Calibrated ages were obtained using the procedure OxCal v3.10.

2.3. Grain Size

Pretreatments for grain-size analysis included subjecting a 0.2–0.4 g sample with H_2O_2 and HCl to remove organic matter and carbonate, respectively. Prior to measurement samples were dispersed with in a $(NaPO_3)_6$ solution and utlrasonics on the machine. The grain-size distribution was measured using a Malvern Mastersizer 2000 laser diffraction instrument. Replicate analyses indicated an analytical error of <2% for the mean grain size.

3. Results

Grain-size data show that loess at both Tongde and Xinghai is typical silt-dominated loess (Figure S2 in Supporting Information S1). More importantly, these data provide insight into the distance that grains travel because grains >20 μm can only be transported within limited height and distance parameters (Pye, 1987). At Tongde 44%–84% of grains and at Xinghai 47%–76% of grains are >20 μm, suggesting that a significant component of the loess is sourced locally and likely from within <100 km.

Results show that most OSL ages are in the correct stratigraphic order, and that they agree well with the radiocarbon age (Tables S1 and S2 in Supporting Information S1). This information, coupled with their favorable response to laboratory tests, indicates the OSL ages have both high accuracy and high precision. Given that sediments collected from <1 m of the ground surface produced ages of >4 ka at multiple sites, it appears that these OSL ages represent the timing of eolian sedimentation, with minimal effects from pedoturbation or other post-depositional processes (Figures 2a–2c). Basal ages from 14 sites indicate that accumulation at individual sites began from 13.8 ± 1.0 to 9.4 ± 0.6 ka (Figures 1b and 2g). Loess stratigraphy and numerical age data indicate that aggradation continued episodically throughout the Holocene, with a soil developed starting at about 8 ka (Figure 2c).

In the Tongde section, 250 cm of loess overlies a gravel layer (Figure S2 in Supporting Information S1), and basal ages suggest that the loess dates to 13.8 ± 1.0 ka at 225 cm depth, and 13.4 ± 1.0 ka at 195 cm depth. Four Holocene ages are found at depths <165 cm. Two samples, both collected from 280 cm depth in the underlying gravel deposits, indicate ages of around 65.5 ± 4.9 and 56.1 ± 4.7 ka. Notably, no loess accumulation during marine isotope stage 2 (MIS 2, ~29–14 ka) is present on the gravel. Similarly, within the Xinghai section 240 cm of loess lies on top of a gravel layer, with basal loess age of 13.2 ± 1.0 ka at the depth of 220 cm. Four Holocene ages were measured in the loess deposited in the upper 175 cm of this deposit. A radiocarbon age of 9820 cal yr BP agrees very well with the OSL age of 9.5 ± 0.7 ka that is found 30 cm below this sample. Of the four Qumalai

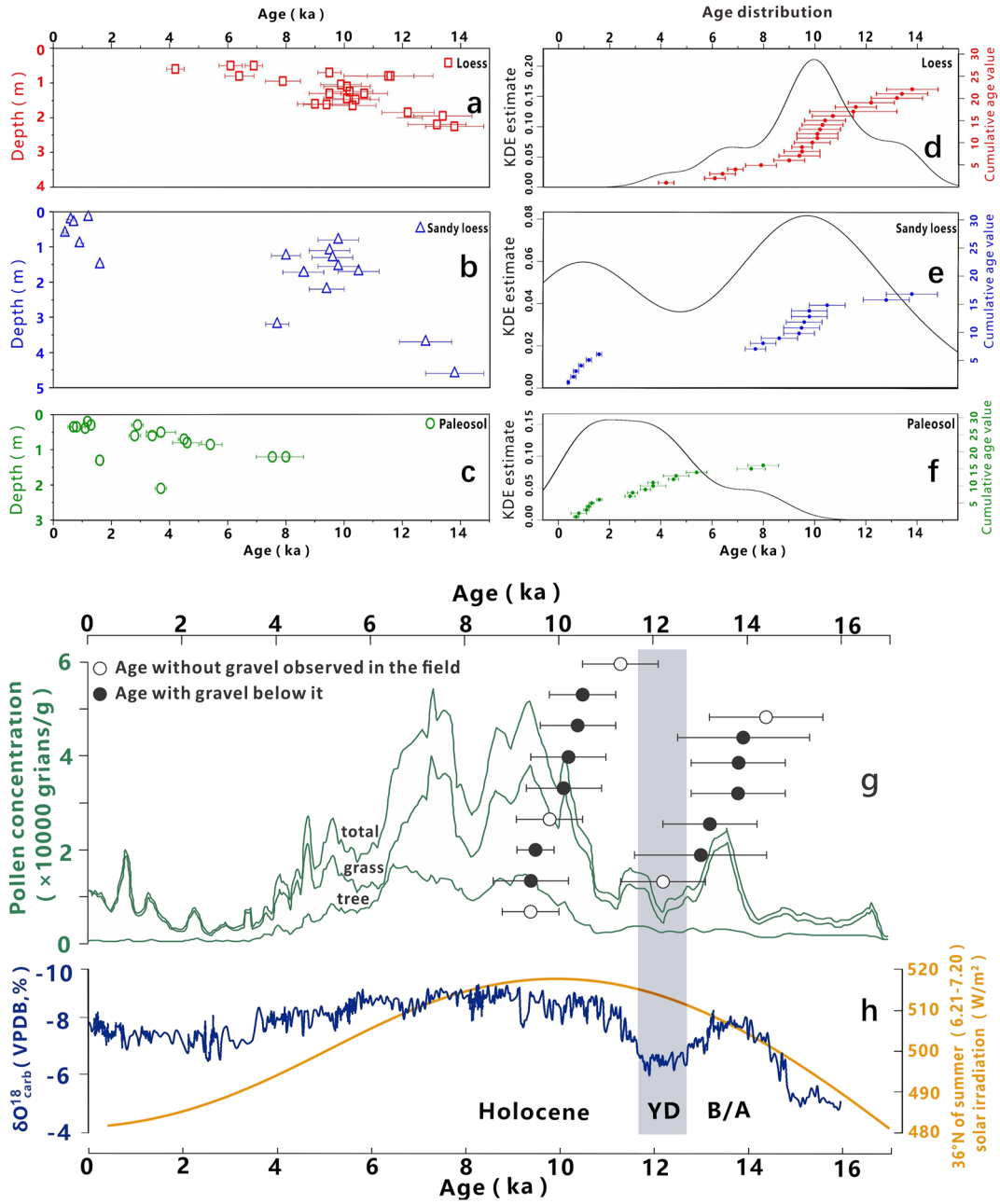

Figure 2. Optically stimulated luminescence (OSL) ages. Ages are classified into loess (a and d), sandy loess (b and e) and paleosol (c and f). Left panels (a to c) are sampling depth versus age; right panels (d to f) are the age probability density functions. Loess ages are clustered at early to mid-Holocene, and paleosol ages mostly date from the mid to late-Holocene. (g and h) Basal OSL ages from 14 sites in comparison to the timing of the Younger Dryas event (gray bar), pollen concentration of Qinghai Lake (green) (Shen et al., 2005) as indication of vegetation cover and ecological responses, solar irradiation (yellow), and oxygen isotope values of Dongge Cave (Dykoski et al., 2005) as indication of precipitation (blue).

sites, different basal ages (from 9.4 ± 0.6 to 13.8 ± 1.0 ka) may suggest that localized factors, such as topographic effects, play a role in the preservation of these dust deposits. More details on the stratigraphy and ages can be found in Figure S1 in the Supporting Information S1.

Our OSL ages are in general agreement with those from previous studies conducted along the Golmud River in the Qaidam Basin (Chen et al., 2011), along the Yarlung Zangbo River in southern TP (Sun et al., 2007) and at two sites near Qinghai Lake (Sun et al., 2017) (Figure 1b). Two groups of basal loess ages are clearly distinct

among all sites including the sites in the three previous studies: we calculated the pooled mean by Calib 8.1, with ages clustered at 13.4 ± 0.4 ka (n = 7) and 9.9 ± 0.2 ka (n = 9) (Figure 1b).

4. Discussion

4.1. Role of Vegetation Cover for Dust Accumulation

We suggest that episodic loess accumulation and preservation in the TP is determined by ecological change, specifically through changes in vegetation cover. Three major factors are required for dust accumulation and preservation: (a) sediment availability from the source area, (b) adequate wind to erode and transport grains, and (c) suitable land surface conditions, such as vegetation cover, to trap the dust (Tsoar & Pye, 1987). Mountain glacial moraines, outwash, debris flow deposits, alluvial fans and braided rivers are common depositional features and landforms in the study area, providing adequate source materials for loess accumulation. Our grain-size data indicate that a significant component of the TP loess is sourced from local sediments (Figure S2 in Supporting Information S1). Wind is not a limiting factor in the interior of the TP, as strong wind and dust storms are observed during the windy seasons of spring and winter under current climate conditions and presumably conditions were similar in the past. Therefore, it is emphasized that change in vegetation cover is the primary ecological factor controlling the accumulation and preservation of the TP loess. This is supported by our data showing that most preserved loess was deposited during the Holocene when increased vegetation cover favored dust trapping, and not during glacial periods such as MIS 2.

Vegetation cover has multiple effects on dust accumulation and preservation (Muhs et al., 2003; Tsoar & Pye, 1987) including: (a) intercepting grains in low suspension transport, (b) increasing the roughness height to slow down wind speeds, and (c) decreasing grain re-entrainment after deposition. During the last glacial maximum, global dust flux increased and led to thick loess deposits in the CLP (upper Malan loess) (Kang et al., 2015; Kohfeld & Harrison, 2003) and the central United States (Peoria loess) (Bettis et al., 2003; Mason et al., 2008; Miao et al., 2018). In contrast, multiple sites show that loess dating to MIS 2 is not preserved in the interior TP. Dust deposition during MIS 2 is recorded in ice cores (Thompson et al., 1989) and lakes (An et al., 2012; Shen et al., 2005) in the TP. However, it was either not trapped on landscapes, or accumulated loess was eroded soon after deposition. “Loess production rates” (source) versus “loess accumulation rates” (sink) were emphasized to differentiate loess stratigraphic models applicable to parts of Alaska and the central USA (Muhs et al., 2003). In Alaska, low vegetation cover did not favor Late Pleistocene loess aggradation, while in the central USA thick Late Pleistocene loess deposits aggraded under conditions in which vegetation cover was adequate. In the TP, increased vegetation cover during the warm Allerød oscillation (~13.4 ± 0.4 ka) caused a major ecological change, favoring the preservation of loess on the landscape (Figure 2h). Therefore, ecological changes in the TP in response to climatic forcing were abrupt in this vegetation-dust-landscape scenario.

4.2. Basal Ages as the Initial Time of Dust Accumulation

In 9 out of 14 sites, basal ages from loess dating to around either 13.4 or 9.9 ka lie directly on the gravel layers (Figures 1b and 2g). These gravel layers are either fluvial deposits on terrace surfaces or alluvial fans or sediment redeposited by outwash from glacial moraines. These relatively flat gravel surfaces not only provide an ideal setting for loess to accumulate, but also serve as a principle stratigraphic marker to represent the onset of loess accumulation. Thus, we interpret the loess basal ages as the times of dramatic ecological and landscape responses to climatic change through a significant increase in vegetation density. Such stratigraphic change is much more straightforward to interpret in climate-landscape interaction than many proxy-based climatic indicators.

This conclusion is supported by comparing our loess chronology with a pollen-based vegetation reconstruction at Qinghai Lake, northeastern TP (Shen et al., 2005) and precipitation reconstructed from speleothems in Dongge Cave (Dykoski et al., 2005) (Figures 2g and 2h). During the LGM, although dust production rates were relatively high, as evidenced by high mineral sedimentation rates at Qinghai Lake and Nam Co, the dominance of sparse vegetation, indicated by the low pollen concentrations in Qinghai Lake, trapped and preserved little loess. Increased vegetation cover due to warming at 13.4 ± 0.4 ka was sufficient to trap and preserve dust to form loess. During Younger Dryas (YD) cooling, loess accumulation at most of our sites stopped, due to reduced vegetation cover, except for sites around Qinghai Lake (Huang et al., 2021; Liu et al., 2012; Sun et al., 2017). Another major episode of loess accumulation began at 9.9 ± 0.2 ka, when pollen concentrations reached one of its highest points

in the Late Quaternary (Shen et al., 2005). Subsequent loess accumulation during the Holocene was also episodic. Although the dating errors of 0.6–1.2 ka of the individual ages make it difficult to investigate the leads and lags before and after the YD event, the pooled mean ages at 13.4 ± 0.4 and 9.9 ± 0.2 ka are offset by 0.8–1.2 ka from the start and end of the YD chronozone. Regardless of any leads or lags, loess deposition in the TP being interrupted by the YD event suggests a profound linkage between abrupt climate forcing and landscape responses, in directions determined by the ecosystem of this cold, dry environment.

4.3. Teleconnections With Northern Hemisphere Climate

Previous studies have established teleconnections between climatic events in the North Atlantic and loess systems in Central Asia (Li et al., 2016) and the CLP (Porter & An, 1995), as well as speleothem isotopic records from Dongge Cave (Dykoski et al., 2005), although a recent study (Walczak et al., 2020) suggests that the Pacific, not the North Atlantic, is the origin of a cascade of dynamic climate events having global impacts. Interpretation of these teleconnections mostly focused on a straightforward link between variability in monsoonal precipitation and loess deposition. However, it is unclear whether such millennial-scale teleconnections are still evident in stratigraphic records involving more complex ecological and landscape responses.

This study offers a clear advantage on this issue. Unlike in Central Asia or the CLP where the loess has major regional sources and conditions in the area of deposition clearly allow accumulation even under relatively cold and dry glacial climates (Kang et al., 2015; Kohfeld & Harrison, 2003; Li et al., 2016), the loess in the TP has localized proximal sources, and dust is deposited in an environment where accumulation and preservation are highly sensitive to the local conditions of the high elevation ecosystem. There is little question that during the last glacial period in the TP climatic conditions were colder and drier than present, and dust transport was widespread, but sparse vegetation cover did not favor loess aggradation. With warming and increased precipitation around 13.4 ± 0.4 ka the ecosystem crossed the threshold that favored dust trapping in at least some locations. This episode of dust accumulation was interrupted by the cold/dry YD event (Figures 2g and 2h) which abruptly and dramatically changed the ecosystem state toward much sparser vegetation. Vegetation recovered afterward and has allowed episodic dust accumulation since 9.9 ka. Thus, we propose a scenario of ecological and landscape responses to abrupt climate change, through complex chain responses from climate forcing to effective moisture, to vegetation response, and to dust capture and loess accumulation, with the patchy loess in turn influencing the present ecosystem and human land use.

4.4. Out-of-Phase Dust Accumulation Models Between TP and CLP

Given the environmental history, it is not surprising that the chronology of dust accumulation in the TP is different, and even out of phase with that in the CLP (Figure 3). In the CLP loess accumulated rapidly under cold climatic conditions such as MIS 2, when loess deposition and preservation was driven by high rates of dust emission and transport by a strong winter monsoon (Kang et al., 2015; Kohfeld & Harrison, 2003). However, loess in the TP aggraded under relatively warm and moist climates when increased vegetation cover were able to trap dust. Loess accumulation was slow and soil formed in the CLP during the early to mid-Holocene due to low rates of dust influx (Figure 3), but moderate dust accumulation occurred at that time in the TP. Finally, soil development occurred in loess deposits of the TP during the mid to late Holocene (starting on ~8 or 5.5 ka, Figure 2c), while loess L0 was deposited in the CLP (Kang et al., 2020), although the transition times between soil formation and predominance of loess accumulation in these two regions may not have been the same. The loess model proposed here for the TP, where vegetation cover and dust trapping in the accumulation area is the key factor rather than climatic control of dust production and transport, is similar to that proposed for central Alaska (Muhs et al., 2003), where loess mostly accumulated during interglacial periods.

The contrasting stratigraphic record of loess in the TP and Loess Plateau can be further understood by considering the effects of internal/external source and sink, and differing sensitivity of dust accumulation to climatic conditions and ecosystem state (Figure 4). Internal, proximal sources of the loess in the TP contrast with external and distal sources for the CLP from upwind arid basins, gobi and sandy lands in northwest China. During climatic warming periods such as the beginning of the Holocene, permafrost thawing in parts of the TP could have increased ecosystem productivity and vegetation cover while also increased erosion rates and stream sediment loads (Li et al., 2021), both potentially favoring dust production and loess accumulation. In contrast, in the CLP,

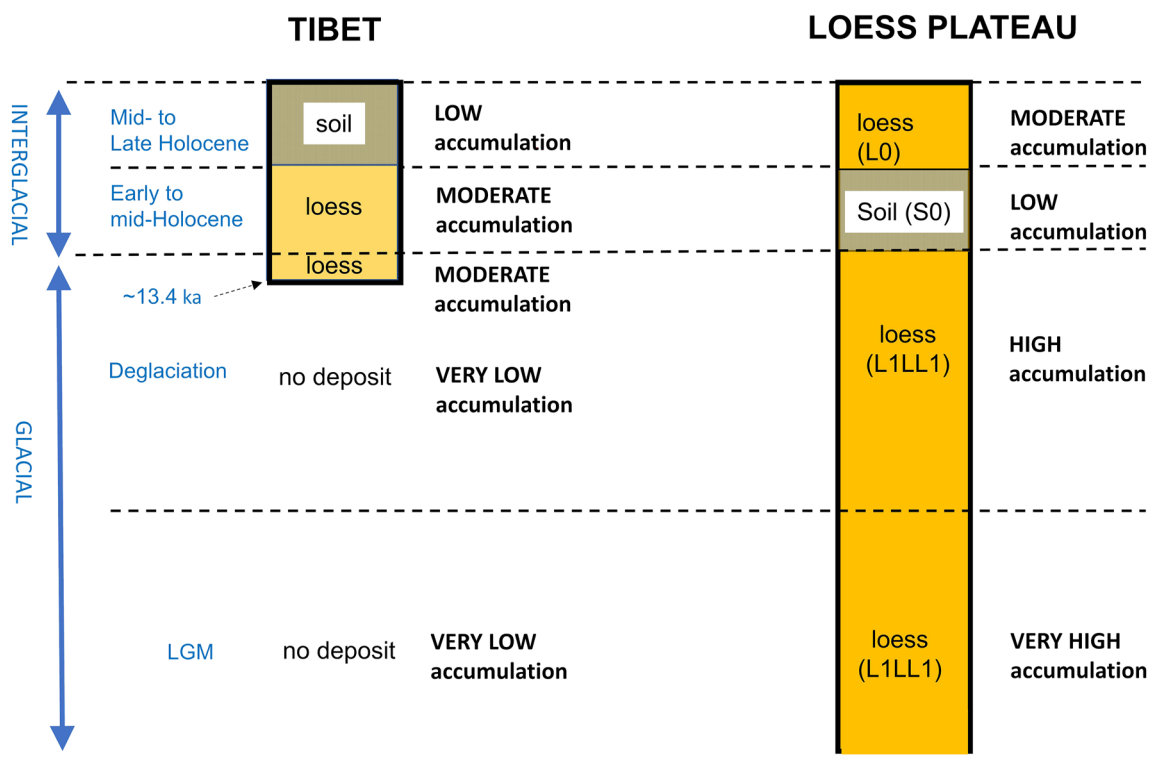

Figure 3. Models of loess stratigraphic diversity in the Tibetan Plateau and Chinese Loess Plateau (CLP) as a function of varying dust accumulation rates during the Late Quaternary. Note the out-of-phase contrasts of landscape change not only at the glacial-interglacial scale, but also within the Holocene. In Holocene, stratigraphy of soil-on-loess in Tibet versus loess-on-soil in the CLP is generalized, although the loess-soil transition time may be different.

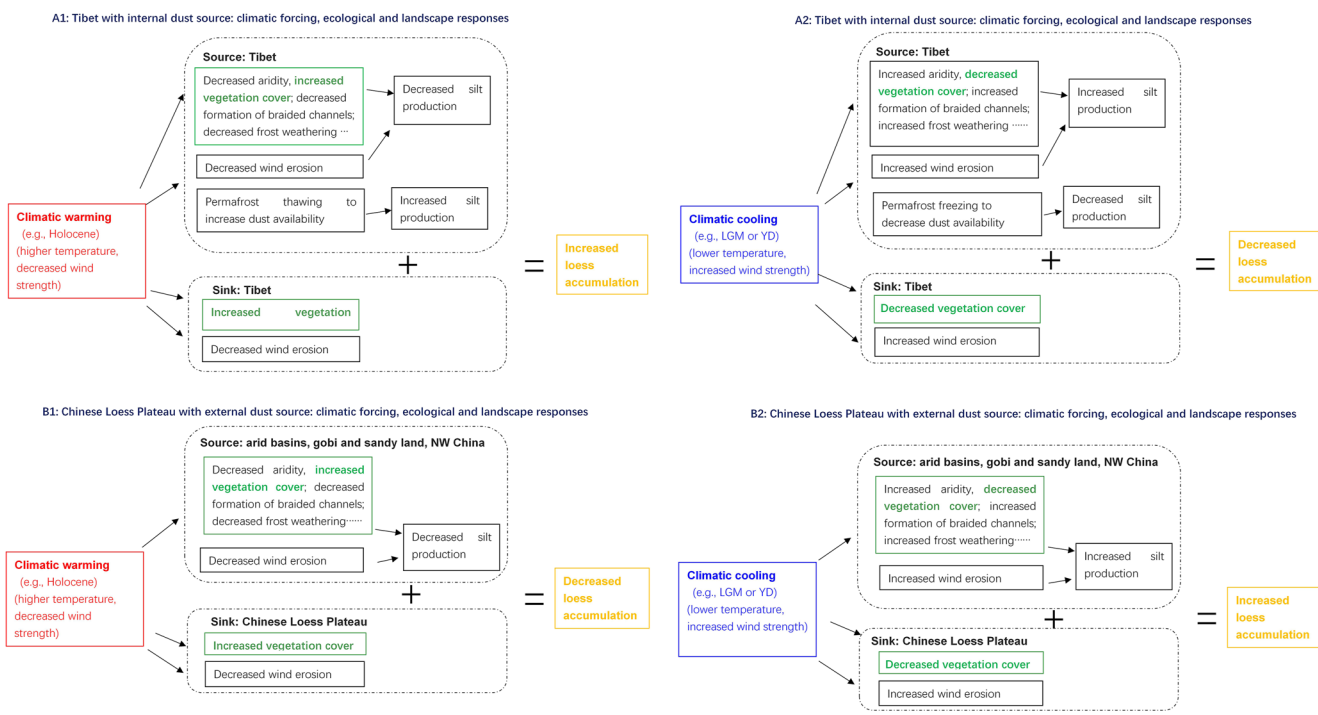

Figure 4. Process-response model of ecological and landscape responses under climatic warming and cooling in the Tibetan Plateau and the Chinese Loess Plateau.

vegetation density in the dust sink is a less important limiting factor for accumulation. Warming and increased precipitation decreased aridity and increased the vegetation cover of the source area for the CLP (Figure 4), decreasing dust production, ultimately reducing loess accumulation instead.

5. Conclusions

Stratigraphic and numerical age data from 14 loess sites covering a large region in the TP enabled us to identify when loess aggradation began and to explore the underlying mechanisms that favored loess accumulation. Results show that the TP loess did not accumulate during the last glacial stage despite the presence of dust in the environment, but began aggrading at either 13.4 ± 0.4 or 9.9 ± 0.2 ka. The basal loess ages are interpreted as the times of dramatic landscape responses to climatic change that resulted in a major increase in vegetation density in favor of loess accumulation. The TP loess was deposited under relatively warm and moist climates, exhibiting a deposition model that is out-of-phase to that of the CLP. Despite being out of phase, loess in the TP and CLP responded to teleconnections associated with late Quaternary Northern Hemispheric climate changes. Unlike the direct link invoked in the CLP between loess deposition and Asian monsoonal precipitation, the TP loess aggraded due to vegetation cover changes driven by climate.

Conflict of Interest

The authors declare no conflicts of interest relevant to this study.

Data Availability Statement

Data reported in this study are available at Figshare via dx.doi.org/10.6084/m9.figshare.16840246. $\delta^{18}O$ data from Dongge Cave speleothem are from Dykoski et al. (2005) and pollen data from Qinghai Lake are from Shen et al. (2005), both of which are used for comparison with the OSL ages.

Acknowledgments
This project was funded by National Natural Science Foundation of China (NSFC 41290252, 42071088), Shantou University (NTF19003), Shandong Provincial Natural Science Foundation (ZR2020MD116), Linyi Univesity (LYDX2018BS058, STKF201929), State Key Laboratory of Loess and Quaternary Geology, Chinese Academy of Sciences (SKLLQG1702). The authors thank Lupeng Yu, Zhixiang Wang, and Yixuan Wang for their assistance in the field, Wanqi Zhao in preparing some of the figures, and William Johnson and an anonymous reviewer for their comments to improve this manuscript.

References

Aitken, M. J. (1998). *An Introduction to Optical Dating*. Oxford University Press.
Alley, R. B., Marotzke, J., Nordhaus, W. D., Overpeck, J. T., Peteet, D. M., Pielke, R. A., et al. (2003). Abrupt climate change. *Science*, *299*(5615), 2005–2010. https://doi.org/10.1126/science.1081056
An, Z., Colman, S. M., Zhou, W., Li, X., Brown, E. T., Jull, A. T., et al. (2012). Interplay between the Westerlies and Asian monsoon recorded in Lake Qinghai sediments since 32 ka. *Scientific Reports*, *2*(1), 1–7. https://doi.org/10.1038/srep00619
Beaumont, L. J., Pitman, A., Perkins, S., Zimmermann, N. E., Yoccoz, N. G., & Thuiller, W. (2011). Impacts of climate change on the world's most exceptional ecoregions. *Proceedings of the National Academy of Sciences*, *108*(6), 2306–2311. https://doi.org/10.1073/pnas.1007217108
Bettis, E. A., Muhs, D. R., Roberts, H. M., & Wintle, A. G. (2003). Last glacial loess in the conterminous USA. *Quaternary Science Reviews*, *22*(18–19), 1907–1946. https://doi.org/10.1016/S0277-3791(03)00169-0
Brown, S. C., Wigley, T. M., Otto-Bliesner, B. L., Rahbek, C., & Fordham, D. A. (2020). Persistent Quaternary climate refugia are hospices for biodiversity in the Anthropocene. *Nature Climate Change*, *10*(3), 244–248. https://doi.org/10.1038/s41558-019-0682-7
Chen, Y., Li, Y., Zhang, Y., Zhang, M., Zhang, J., Yi, C., & Liu, G. (2011). Late Quaternary deposition and incision sequences of the Golmud River and their environmental implications. *Quaternary International*, *236*(1–2), 48–56. https://doi.org/10.1016/j.quaint.2010.05.028
Duller, G. (2003). Distinguishing quartz and feldspar in single grain luminescence measurements. *Radiation Measurements*, *37*(2), 161–165. https://doi.org/10.1016/S1350-4487(02)00170-1
Durcan, J. A., King, G. E., & Duller, G. A. (2015). DRAC: Dose rate and age calculator for trapped charge dating. *Quaternary Geochronology*, *28*, 54–61. https://doi.org/10.1016/j.quageo.2015.03.012
Dykoski, C. A., Edwards, R. L., Cheng, H., Yuan, D., Cai, Y., Zhang, M., et al. (2005). A high-resolution, absolute-dated Holocene and deglacial Asian monsoon record from Dongge Cave, China. *Earth and Planetary Science Letters*, *233*(1–2), 71–86. https://doi.org/10.1016/j.epsl.2005.01.036
Galbraith, R. F., & Roberts, R. G. (2012). Statistical aspects of equivalent dose and error calculation and display in OSL dating: An overview and some recommendations. *Quaternary Geochronology*, *11*, 1–27. https://doi.org/10.1016/j.quageo.2012.04.020
Huang, C., Lai, Z., Liu, X., & Madsen, D. (2021). Lake-level history of Qinghai Lake on the NE Tibetan Plateau and its implications for Asian monsoon pattern - A review. *Quaternary Science Reviews*, *273*, 107258. https://doi.org/10.1016/j.quascirev.2021.107258
Joshi, M., Hawkins, E., Sutton, R., Lowe, J., & Frame, D. (2011). Projections of when temperature change will exceed 2°C above pre-industrial levels. *Nature Climate Change*, *1*(8), 407–412. https://doi.org/10.1038/nclimate1261
Kang, S., Du, J., Wang, N., Dong, J., Wang, D., Wang, X., et al. (2020). Early Holocene weakening and mid- to late Holocene strengthening of the East Asian winter monsoon. *Geology*, *48*, 1043–1047. https://doi.org/10.1130/G47621.1
Kang, S., Roberts, H. M., Wang, X., An, Z., & Wang, M. (2015). Mass accumulation rate changes in Chinese loess during MIS 2, and asynchrony with records from Greenland ice cores and North Pacific Ocean sediments during the Last Glacial Maximum. *Aeolian Research*, *19*, 251–258. https://doi.org/10.1016/j.aeolia.2015.05.005
Kohfeld, K., & Harrison, S. (2003). Glacial-interglacial changes in dust deposition on the Chinese Loess Plateau. *Quaternary Science Reviews*, *22*(18–19), 1859–1878. https://doi.org/10.1016/s0277-3791(03)00166-5

Lai, Z. (2006). Testing the use of an OSL standardised growth curve (SGC) for De determination on quartz from the Chinese Loess Plateau. *Radiation Measurements*, *41*(1), 9–16. https://doi.org/10.1016/j.radmeas.2005.06.031

Lai, Z. (2010). Chronology and the upper dating limit for loess samples from Luochuan section in the Chinese Loess Plateau using quartz OSL SAR protocol. *Journal of Asian Earth Sciences*, *37*(2), 176–185. https://doi.org/10.1016/j.jseaes.2009.08.003

Lai, Z., & Brueckner, H. (2008). Effects of feldspar contamination on equivalent dose and the shape of growth curve for OSL of silt-sized quartz extracted from Chinese loess. *Geochronometria*, *30*(1), 49–53. https://doi.org/10.2478/v10003-008-0010-0

Lai, Z., Kaiser, K., & Brückner, H. (2009). Luminescence-dated aeolian deposits of late Quaternary age in the southern Tibetan Plateau and their implications for landscape history. *Quaternary Research*, *72*(3), 421–430. https://doi.org/10.1016/j.yqres.2009.07.005

Lai, Z., & Wintle, A. G. (2006). Locating the boundary between the Pleistocene and the Holocene in Chinese loess using luminescence. *The Holocene*, *16*(6), 893–899. https://doi.org/10.1191/0959683606hol980rr

Lai, Z., Zöller, L., Fuchs, M., & Brückner, H. (2008). Alpha efficiency determination for OSL of quartz extracted from Chinese loess. *Radiation Measurements*, *43*(2–6), 767–770. https://doi.org/10.1016/j.radmeas.2008.01.022

Lenton, T. M., Held, H., Kriegler, E., Hall, J. W., Lucht, W., Rahmstorf, S., & Schellnhuber, H. J. (2008). Tipping elements in the Earth's climate system. *Proceedings of the National Academy of Sciences*, *105*(6), 1786–1793. https://doi.org/10.1073/pnas.0705414105

Li, D., Overeem, I., Kettner, A. J., Zhou, Y., & Xixi, L. (2021). Air temperature regulates erodible landscape, water and sediment fluxes in the permafrost-dominated catchment on the Tibetan Plateau. *Water Resources Research*, *57*, e2020WR028193. https://doi.org/10.1029/2020WR028193

Li, Y., Song, Y., Lai, Z., Han, L., & An, Z. (2016). Rapid and cyclic dust accumulation during MIS 2 in Central Asia inferred from loess OSL dating and grain-size analysis. *Scientific Reports*, *6*(1), 1–6. https://doi.org/10.1038/srep32365

Liu, X., & Chen, B. (2000). Climatic warming in the Tibetan Plateau during recent decades. *International Journal of Climatology*, *20*(14), 1729–1742. https://doi.org/10.1002/1097-0088(20001130)20:14<1729::aid-joc556>3.0.co;2-y

Liu, X., Lai, Z., Yu, L., Sun, Y., & Madsen, D. (2012). Luminescence chronology of aeolian deposits from the Qinghai Lake area in the Northeastern Qinghai-Tibetan Plateau and its palaeoenvironmental implications. *Quaternary Geochronology*, *10*, 37–43. https://doi.org/10.1016/j.quageo.2012.01.016

Lu, H., Wang, X., An, Z., Miao, X., Zhu, R., Ma, H., et al. (2004). Geomorphologic evidence of phased uplift of the northeastern Qinghai-Tibet Plateau since 14 million years ago. *Science in China - Series D: Earth Sciences*, *47*, 822–833. https://doi.org/10.1360/03yd0315

Mason, J. A., Miao, X., Hanson, P. R., Johnson, W. C., Jacobs, P. M., & Goble, R. J. (2008). Loess record of the Pleistocene–Holocene transition on the northern and central Great Plains, USA. *Quaternary Science Reviews*, *27*(17–18), 1772–1783. https://doi.org/10.1016/j.quascirev.2008.07.004

Miao, X., Hanson, P. R., Stohr, C. J., & Wang, H. (2018). Holocene loess in Illinois revealed by OSL dating: Implications for stratigraphy and geoarchaeology of the Midwest United States. *Quaternary Science Reviews*, *200*(15), 253–261. https://doi.org/10.1016/j.quascirev.2018.09.039

Muhs, D. R., Ager, T. A., Bettis, E. A., III, McGeehin, J., Been, J. M., Begét, J. E., et al. (2003). Stratigraphy and palaeoclimatic significance of Late Quaternary loess–palaeosol sequences of the Last Interglacial–Glacial cycle in central Alaska. *Quaternary Science Reviews*, *22*(18–19), 1947–1986. https://doi.org/10.1016/s0277-3791(03)00167-7

Murray, A. S., & Wintle, A. G. (2000). Luminescence dating of quartz using an improved single-aliquot regenerative-dose protocol. *Radiation Measurements*, *32*(1), 57–73. https://doi.org/10.1016/S1350-4487(99)00253-X

Porter, S. C., & An, Z. (1995). Correlation between climate events in the North Atlantic and China during the last glaciation. *Nature*, *375*(6529), 305–308. https://doi.org/10.1038/375305a0

Prescott, J. R., & Hutton, J. T. (1994). Cosmic ray contributions to dose rates for luminescence and ESR dating: Large depths and long-term time variations. *Radiation Measurements*, *23*(2–3), 497–500. https://doi.org/10.1016/1350-4487(94)90086-8

Pye, K. (1987). *Aeolian dust and dust deposits*. Academic Press.

Roberts, H., & Duller, G. A. (2004). Standardised growth curves for optical dating of sediment using multiple-grain aliquots. *Radiation Measurements*, *38*(2), 241–252. https://doi.org/10.1016/j.radmeas.2003.10.001

Shen, J., Liu, X., Wang, S., & Matsumoto, R. (2005). Palaeoclimatic changes in the Qinghai Lake area during the last 18,000 years. *Quaternary International*, *136*(1), 131–140. https://doi.org/10.1016/j.quaint.2004.11.014

Stauch, G. (2015). Geomorphological and palaeoclimate dynamics recorded by the formation of aeolian archives on the Tibetan Plateau. *Earth-Science Reviews*, *150*, 393–408. https://doi.org/10.1016/j.earscirev.2015.08.009

Steinbauer, M. J., Grytnes, J.-A., Jurasinski, G., Kulonen, A., Lenoir, J., Pauli, H., et al. (2018). Accelerated increase in plant species richness on mountain summits is linked to warming. *Nature*, *556*(7700), 231–234. https://doi.org/10.1038/s41586-018-0005-6

Sun, J., Li, S.-H., Muhs, D. R., & Li, B. (2007). Loess sedimentation in Tibet: Provenance, processes, and link with Quaternary glaciations. *Quaternary Science Reviews*, *26*(17–18), 2265–2280. https://doi.org/10.1016/j.quascirev.2007.05.003

Sun, Y., Chongyi, E., Lai, Z., & Hou, G. (2017). Luminescence dating of prehistoric hearths in Northeast Qinghai Lake and its paleoclimatic implication. *Archaeological and Anthropological Sciences*, *10*(6), 1525–1534. https://doi.org/10.1007/s12520-017-0472-y

Thompson, L. G., Mosley-Thompson, E., Davis, M., Bolzan, J., Dai, J., Klein, L., et al. (1989). Holocene—Late Pleistocene climatic ice core records from Qinghai-Tibetan Plateau. *Science*, *246*(4929), 474–477. https://doi.org/10.1126/science.246.4929.474

Tsoar, H., & Pye, K. (1987). Dust transport and the question of desert loess formation. *Sedimentology*, *34*(1), 139–153. https://doi.org/10.1111/j.1365-3091.1987.tb00566.x

Walczak, M. H., Mix, A. C., Cowan, E. A., Fallon, S., Fifield, L. K., Alder, J. R., et al. (2020). Phasing of millennial-scale climate variability in the Pacific and Atlantic oceans. *Science*, *370*(6517), 716–720. https://doi.org/10.1126/science.aba7096

Williams, J. W., Ordonez, A., & Svenning, J.-C. (2021). A unifying framework for studying and managing climate-driven rates of ecological change. *Nature Ecology & Evolution*, *5*(1), 17–26. https://doi.org/10.1038/s41559-020-01344-5

Yang, S., Liu, L., Chen, H., Tang, G., Luo, Y., Liu, N., et al. (2021). Variability and environmental significance of organic carbon isotopes in Ganzi loess since the last interglacial on the eastern Tibetan Plateau. *Catena*, *196*, 104866. https://doi.org/10.1016/j.catena.2020.104866